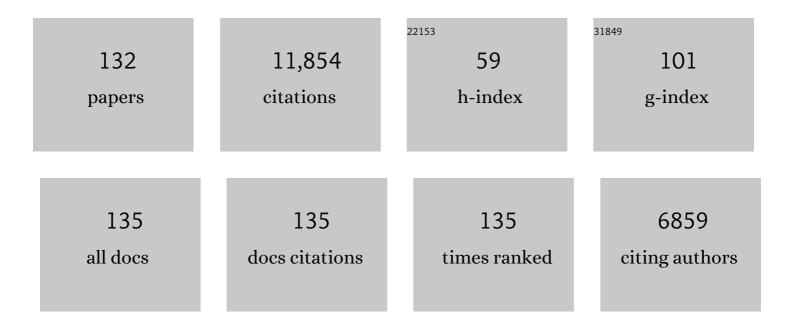
Scot Martin

List of Publications by Year in descending order

Source: https://exaly.com/author-pdf/6700692/publications.pdf Version: 2024-02-01



#	Article	IF	CITATIONS
1	How do aerosols above the residual layer affect the planetary boundary layer height?. Science of the Total Environment, 2022, 814, 151953.	8.0	30
2	Tight Coupling of Surface and In-Plant Biochemistry and Convection Governs Key Fine Particulate Components over the Amazon Rainforest. ACS Earth and Space Chemistry, 2022, 6, 380-390.	2.7	11
3	Reconciling Observed and Predicted Tropical Rainforest OH Concentrations. Journal of Geophysical Research D: Atmospheres, 2022, 127, .	3.3	6
4	Phase Behavior of Internal Mixtures of Hydrocarbon-like Primary Organic Aerosol and Secondary Aerosol Based on Their Differences in Oxygen-to-Carbon Ratios. Environmental Science & Technology, 2022, 56, 3960-3973.	10.0	12
5	Assessing the Nonlinear Effect of Atmospheric Variables on Primary and Oxygenated Organic Aerosol Concentration Using Machine Learning. ACS Earth and Space Chemistry, 2022, 6, 1059-1066.	2.7	8
6	Partitioning of Organonitrates in the Production of Secondary Organic Aerosols from α-Pinene Photo-Oxidation. Environmental Science & Technology, 2022, 56, 5421-5429.	10.0	4
7	Liquid-liquid phase separation reduces radiative absorption by aged black carbon aerosols. Communications Earth & Environment, 2022, 3, .	6.8	16
8	River Winds and Transport of Forest Volatiles in the Amazonian Riparian Ecoregion. Environmental Science & Technology, 2022, 56, 12667-12677.	10.0	4
9	Near-canopy horizontal concentration heterogeneity of semivolatile oxygenated organic compounds and implications for 2-methyltetrols primary emissions. Environmental Science Atmospheres, 2021, 1, 8-20.	2.4	4
10	Unmanned Aerial Vehicle Measurements of Volatile Organic Compounds over a Subtropical Forest in China and Implications for Emission Heterogeneity. ACS Earth and Space Chemistry, 2021, 5, 247-256.	2.7	8
11	Aqueous production of secondary organic aerosol from fossil-fuel emissions in winter Beijing haze. Proceedings of the National Academy of Sciences of the United States of America, 2021, 118, .	7.1	75
12	Optimization and Representativeness of Atmospheric Chemical Sampling by Hovering Unmanned Aerial Vehicles Over Tropical Forests. Earth and Space Science, 2021, 8, e2020EA001335.	2.6	8
13	Fluorescence Aerosol Flow Tube Spectroscopy to Detect Liquid–Liquid Phase Separation. ACS Earth and Space Chemistry, 2021, 5, 1223-1232.	2.7	18
14	Humidity Dependence of the Condensational Growth of α-Pinene Secondary Organic Aerosol Particles. Environmental Science & Technology, 2021, 55, 14360-14369.	10.0	15
15	River winds and pollutant recirculation near the Manaus city in the central Amazon. Communications Earth & Environment, 2021, 2, .	6.8	8
16	Enhanced aerosol particle growth sustained by high continental chlorine emission in India. Nature Geoscience, 2021, 14, 77-84.	12.9	94
17	Chemical Characterization and Source Apportionment of Organic Aerosols in the Coastal City of Chennai, India: Impact of Marine Air Masses on Aerosol Chemical Composition and Potential for Secondary Organic Aerosol Formation. ACS Earth and Space Chemistry, 2021, 5, 3197-3209.	2.7	12
18	Temperature-Dependent Viscosity of Organic Materials Characterized by Atomic Force Microscope. Atmosphere, 2021, 12, 1476.	2.3	3

#	Article	IF	CITATIONS
19	Planetary Boundary Layer Height Modulates Aerosol—Water Vapor Interactions During Winter in the Megacity of Delhi. Journal of Geophysical Research D: Atmospheres, 2021, 126, e2021JD035681.	3.3	4
20	Vertical profiling of fine particulate matter and black carbon by using unmanned aerial vehicle in Macau, China. Science of the Total Environment, 2020, 709, 136109.	8.0	39
21	Synergistic Uptake by Acidic Sulfate Particles of Gaseous Mixtures of Glyoxal and Pinanediol. Environmental Science & Technology, 2020, 54, 11762-11770.	10.0	5
22	Vertical Profiles of Atmospheric Species Concentrations and Nighttime Boundary Layer Structure in the Dry Season over an Urban Environment in Central Amazon Collected by an Unmanned Aerial Vehicle. Atmosphere, 2020, 11, 1371.	2.3	13
23	The Stove, Dome, and Umbrella Effects of Atmospheric Aerosol on the Development of the Planetary Boundary Layer in Hazy Regions. Geophysical Research Letters, 2020, 47, e2020GL087373.	4.0	73
24	Fast sulfate formation from oxidation of SO2 by NO2 and HONO observed in Beijing haze. Nature Communications, 2020, 11, 2844.	12.8	161
25	Comparison of aircraft measurements during GoAmazon2014/5 and ACRIDICON-CHUVA. Atmospheric Measurement Techniques, 2020, 13, 661-684.	3.1	12
26	Interactions Between the Amazonian Rainforest andÂCumuli Clouds: A Largeâ€Eddy Simulation, Highâ€Resolution ECMWF, and Observational Intercomparison Study. Journal of Advances in Modeling Earth Systems, 2020, 12, e2019MS001828.	3.8	10
27	Leaf isoprene and monoterpene emission distribution across hyperdominant tree genera in the Amazon basin. Phytochemistry, 2020, 175, 112366.	2.9	21
28	Natural and Anthropogenically Influenced Isoprene Oxidation in Southeastern United States and Central Amazon. Environmental Science & Technology, 2020, 54, 5980-5991.	10.0	22
29	New SOA Treatments Within the Energy Exascale Earth System Model (E3SM): Strong Production and Sinks Govern Atmospheric SOA Distributions and Radiative Forcing. Journal of Advances in Modeling Earth Systems, 2020, 12, e2020MS002266.	3.8	15
30	Synthesis and surface spectroscopy of $\hat{l}\pm$ -pinene isotopologues and their corresponding secondary organic material. Chemical Science, 2019, 10, 8390-8398.	7.4	8
31	A sampler for atmospheric volatile organic compounds by copter unmanned aerial vehicles. Atmospheric Measurement Techniques, 2019, 12, 3123-3135.	3.1	40
32	Contributions of biomass-burning, urban, and biogenic emissions to the concentrations and light-absorbing properties of particulate matter in central Amazonia during the dry season. Atmospheric Chemistry and Physics, 2019, 19, 7973-8001.	4.9	36
33	Quantifying the Role of the Relative Humidity-Dependent Physical State of Organic Particulate Matter in the Uptake of Semivolatile Organic Molecules. Environmental Science & Technology, 2019, 53, 13209-13218.	10.0	16
34	Intermediate-scale horizontal isoprene concentrations in the near-canopy forest atmosphere and implications for emission heterogeneity. Proceedings of the National Academy of Sciences of the United States of America, 2019, 116, 19318-19323.	7.1	28
35	Vertical Profiles of Ozone Concentration Collected by an Unmanned Aerial Vehicle and the Mixing of the Nighttime Boundary Layer over an Amazonian Urban Area. Atmosphere, 2019, 10, 599.	2.3	21
36	Increasing Isoprene Epoxydiol-to-Inorganic Sulfate Aerosol Ratio Results in Extensive Conversion of Inorganic Sulfate to Organosulfur Forms: Implications for Aerosol Physicochemical Properties. Environmental Science & Technology, 2019, 53, 8682-8694.	10.0	111

#	Article	IF	CITATIONS
37	Urban pollution greatly enhances formation of natural aerosols over the Amazon rainforest. Nature Communications, 2019, 10, 1046.	12.8	131
38	Atmospheric β-Caryophyllene-Derived Ozonolysis Products at Interfaces. ACS Earth and Space Chemistry, 2019, 3, 158-169.	2.7	10
39	The viscosity of atmospherically relevant organic particles. Nature Communications, 2018, 9, 956.	12.8	252
40	Isoprene photo-oxidation products quantify the effect of pollution on hydroxyl radicals over Amazonia. Science Advances, 2018, 4, eaar2547.	10.3	28
41	Highly Viscous States Affect the Browning of Atmospheric Organic Particulate Matter. ACS Central Science, 2018, 4, 207-215.	11.3	60
42	Growth Kinetics and Size Distribution Dynamics of Viscous Secondary Organic Aerosol. Environmental Science & Technology, 2018, 52, 1191-1199.	10.0	85
43	Aircraft-based observations of isoprene-epoxydiol-derived secondary organic aerosol (IEPOX-SOA) in the tropical upper troposphere over the Amazon region. Atmospheric Chemistry and Physics, 2018, 18, 14979-15001.	4.9	39
44	Production and Measurement of Organic Particulate Matter in a Flow Tube Reactor. Journal of Visualized Experiments, 2018, , .	0.3	4
45	Organosulfates in aerosols downwind of an urban region in central Amazon. Environmental Sciences: Processes and Impacts, 2018, 20, 1546-1558.	3.5	40
46	Resolving the mechanisms of hygroscopic growth and cloud condensation nuclei activity for organic particulate matter. Nature Communications, 2018, 9, 4076.	12.8	84
47	Development of a hydrophilic interaction liquid chromatography (HILIC) method for the chemical characterization of water-soluble isoprene epoxydiol (IEPOX)-derived secondary organic aerosol. Environmental Sciences: Processes and Impacts, 2018, 20, 1524-1536.	3.5	66
48	Long-term observations of cloud condensation nuclei over the Amazon rain forest – Part 2: Variability and characteristics of biomass burning, long-range transport, and pristine rain forest aerosols. Atmospheric Chemistry and Physics, 2018, 18, 10289-10331.	4.9	64
49	Observations of sesquiterpenes and their oxidation products in central Amazonia during the wet and dry seasons. Atmospheric Chemistry and Physics, 2018, 18, 10433-10457.	4.9	53
50	Biomass burning and carbon monoxide patterns in Brazil during the extreme drought years of 2005, 2010, and 2015. Environmental Pollution, 2018, 243, 1008-1014.	7.5	30
51	Aircraft observations of the chemical composition and aging of aerosol in the Manaus urban plume during GoAmazon 2014/5. Atmospheric Chemistry and Physics, 2018, 18, 10773-10797.	4.9	32
52	Influence of Particle Physical State on the Uptake of Medium-Sized Organic Molecules. Environmental Science & Technology, 2018, 52, 8381-8389.	10.0	11
53	Urban influence on the concentration and composition of submicron particulate matter in central Amazonia. Atmospheric Chemistry and Physics, 2018, 18, 12185-12206.	4.9	30
54	Rebounding hygroscopic inorganic aerosol particles: Liquids, gels, and hydrates. Aerosol Science and Technology, 2017, 51, 388-396.	3.1	36

#	Article	IF	CITATIONS
55	Airborne observations reveal elevational gradient in tropical forest isoprene emissions. Nature Communications, 2017, 8, 15541.	12.8	53
56	Cloud Activation Potentials for Atmospheric α-Pinene and β-Caryophyllene Ozonolysis Products. ACS Central Science, 2017, 3, 715-725.	11.3	40
57	The Green Ocean Amazon Experiment (GoAmazon2014/5) Observes Pollution Affecting Gases, Aerosols, Clouds, and Rainfall over the Rain Forest. Bulletin of the American Meteorological Society, 2017, 98, 981-997.	3.3	128
58	Influence of urban pollution on the production of organic particulate matter from isoprene epoxydiols in central Amazonia. Atmospheric Chemistry and Physics, 2017, 17, 6611-6629.	4.9	45
59	Cloud characteristics, thermodynamic controls and radiative impacts during the Observations and Modeling of the Green Ocean Amazon (GoAmazon2014/5) experiment. Atmospheric Chemistry and Physics, 2017, 17, 14519-14541.	4.9	38
60	Illustration of microphysical processes in Amazonian deep convective clouds in the gamma phase space: introduction and potential applications. Atmospheric Chemistry and Physics, 2017, 17, 14727-14746.	4.9	8
61	Contributions of mobile, stationary and biogenic sources to air pollution in the Amazon rainforest: a numerical study with the WRF-Chem model. Atmospheric Chemistry and Physics, 2017, 17, 7977-7995.	4.9	45
62	Power plant fuel switching and air quality in a tropical, forested environment. Atmospheric Chemistry and Physics, 2017, 17, 8987-8998.	4.9	28
63	Recent advances in understanding secondary organic aerosol: Implications for global climate forcing. Reviews of Geophysics, 2017, 55, 509-559.	23.0	548
64	Isoprene photochemistry over the Amazon rainforest. Proceedings of the National Academy of Sciences of the United States of America, 2016, 113, 6125-6130.	7.1	85
65	Optical Properties of Secondary Organic Aerosol from <i>cis</i> -3-Hexenol and <i>cis</i> -3-Hexenyl Acetate: Effect of Chemical Composition, Humidity, and Phase. Environmental Science & Technology, 2016, 50, 4997-5006.	10.0	15
66	Ambient Gas-Particle Partitioning of Tracers for Biogenic Oxidation. Environmental Science & Technology, 2016, 50, 9952-9962.	10.0	69
67	Lability of secondary organic particulate matter. Proceedings of the National Academy of Sciences of the United States of America, 2016, 113, 12643-12648.	7.1	93
68	Introduction: Observations and Modeling of the Green Ocean Amazon (GoAmazon2014/5). Atmospheric Chemistry and Physics, 2016, 16, 4785-4797.	4.9	213
69	Effect of varying experimental conditions on the viscosity of <i>α</i> -pinene derived secondary organic material. Atmospheric Chemistry and Physics, 2016, 16, 6027-6040.	4.9	79
70	Volatility and lifetime against OH heterogeneous reaction of ambient isoprene-epoxydiols-derived secondary organic aerosol (IEPOX-SOA). Atmospheric Chemistry and Physics, 2016, 16, 11563-11580.	4.9	82
71	Long-term observations of cloud condensation nuclei in the Amazon rain forest – Part 1: Aerosol size distribution, hygroscopicity, and new model parametrizations for CCN prediction. Atmospheric Chemistry and Physics, 2016, 16, 15709-15740.	4.9	105
72	Observations and implications of liquid–liquid phase separation at high relative humidities in secondary organic material produced by <l>l±-pinene ozonolysis without inorganic salts. Atmospheric Chemistry and Physics, 2016, 16, 7969-7979.</l>	4.9	93

#	Article	IF	CITATIONS
73	Relative humidity-dependent viscosity of secondary organic material from toluene photo-oxidation and possible implications for organic particulate matter over megacities. Atmospheric Chemistry and Physics, 2016, 16, 8817-8830.	4.9	95
74	ACRIDICON–CHUVA Campaign: Studying Tropical Deep Convective Clouds and Precipitation over Amazonia Using the New German Research Aircraft HALO. Bulletin of the American Meteorological Society, 2016, 97, 1885-1908.	3.3	124
75	Spatial Variability of the Background Diurnal Cycle of Deep Convection around the GoAmazon2014/5 Field Campaign Sites. Journal of Applied Meteorology and Climatology, 2016, 55, 1579-1598.	1.5	38
76	Sub-micrometre particulate matter is primarily in liquid form over Amazon rainforest. Nature Geoscience, 2016, 9, 34-37.	12.9	99
77	Uptake and release of gaseous species accompanying the reactions of isoprene photo-oxidation products with sulfate particles. Physical Chemistry Chemical Physics, 2016, 18, 1595-1600.	2.8	20
78	Dimethyl sulfide in the Amazon rain forest. Global Biogeochemical Cycles, 2015, 29, 19-32.	4.9	58
79	Ultraviolet and visible complex refractive indices of secondary organic material produced by photooxidation of the aromatic compounds toluene and <i>m</i> -xylene. Atmospheric Chemistry and Physics, 2015, 15, 1435-1446.	4.9	121
80	Submicron particle mass concentrations and sources in the Amazonian wet season (AMAZE-08). Atmospheric Chemistry and Physics, 2015, 15, 3687-3701.	4.9	88
81	Examining the effects of anthropogenic emissions on isoprene-derived secondary organic aerosol formation during the 2013 Southern Oxidant and Aerosol Study (SOAS) at the Look Rock, Tennessee ground site. Atmospheric Chemistry and Physics, 2015, 15, 8871-8888.	4.9	213
82	Characterization of a real-time tracer for isoprene epoxydiols-derived secondary organic aerosol (IEPOX-SOA) from aerosol mass spectrometer measurements. Atmospheric Chemistry and Physics, 2015, 15, 11807-11833.	4.9	185
83	A synthesis of cloud condensation nuclei counter (CCNC) measurements within the EUCAARI network. Atmospheric Chemistry and Physics, 2015, 15, 12211-12229.	4.9	58
84	Changing shapes and implied viscosities of suspended submicron particles. Atmospheric Chemistry and Physics, 2015, 15, 7819-7829.	4.9	106
85	Elemental composition of organic aerosol: The gap between ambient and laboratory measurements. Geophysical Research Letters, 2015, 42, 4182-4189.	4.0	84
86	Green Leaf Volatile Emissions during High Temperature and Drought Stress in a Central Amazon Rainforest. Plants, 2015, 4, 678-690.	3.5	41
87	Highly reactive lightâ€dependent monoterpenes in the Amazon. Geophysical Research Letters, 2015, 42, 1576-1583.	4.0	71
88	Physical state and acidity of inorganic sulfate can regulate the production of secondary organic material from isoprene photooxidation products. Physical Chemistry Chemical Physics, 2015, 17, 5670-5678.	2.8	30
89	On Surface Order and Disorder of α-Pinene-Derived Secondary Organic Material. Journal of Physical Chemistry A, 2015, 119, 4609-4617.	2.5	27
90	Hygroscopic Influence on the Semisolid-to-Liquid Transition of Secondary Organic Materials. Journal of Physical Chemistry A, 2015, 119, 4386-4395.	2.5	112

#	Article	IF	CITATIONS
91	Uptake of Epoxydiol Isomers Accounts for Half of the Particle-Phase Material Produced from Isoprene Photooxidation via the HO ₂ Pathway. Environmental Science & Technology, 2015, 49, 250-258.	10.0	48
92	Chemical Reactivity and Liquid/Nonliquid States of Secondary Organic Material. Environmental Science & Technology, 2015, 49, 13264-13274.	10.0	74
93	Impactor Apparatus for the Study of Particle Rebound: Relative Humidity and Capillary Forces. Aerosol Science and Technology, 2014, 48, 42-52.	3.1	91
94	An Analytic Equation for the Volume Fraction of Condensationally Grown Mixed Particles and Applications to Secondary Organic Material Produced in Continuously Mixed Flow Reactors. Aerosol Science and Technology, 2014, 48, 803-812.	3.1	5
95	Liquid–liquid phase separation in atmospherically relevant particles consisting of organic species and inorganic salts. International Reviews in Physical Chemistry, 2014, 33, 43-77.	2.3	160
96	Trends in sulfate and organic aerosol mass in the Southeast U.S.: Impact on aerosol optical depth and radiative forcing. Geophysical Research Letters, 2014, 41, 7701-7709.	4.0	77
97	Complex Refractive Indices of Thin Films of Secondary Organic Materials by Spectroscopic Ellipsometry from 220 to 1200 nm. Environmental Science & Technology, 2013, 47, 13594-13601.	10.0	85
98	Vibrational Sum Frequency Generation Spectroscopy of Secondary Organic Material Produced by Condensational Growth from α-Pinene Ozonolysis. Journal of Physical Chemistry A, 2013, 117, 8427-8436.	2.5	29
99	Viscosity of <i>α</i> -pinene secondary organic material and implications for particle growth and reactivity. Proceedings of the National Academy of Sciences of the United States of America, 2013, 110, 8014-8019.	7.1	388
100	Production of methyl vinyl ketone and methacrolein via the hydroperoxyl pathway of isoprene oxidation. Atmospheric Chemistry and Physics, 2013, 13, 5715-5730.	4.9	141
101	Particle Size Distributions following Condensational Growth in Continuous Flow Aerosol Reactors as Derived from Residence Time Distributions: Theoretical Development and Application to Secondary Organic Aerosol. Aerosol Science and Technology, 2012, 46, 937-949.	3.1	22
102	Images reveal that atmospheric particles can undergo liquid–liquid phase separations. Proceedings of the United States of America, 2012, 109, 13188-13193.	7.1	205
103	Phase of atmospheric secondary organic material affects its reactivity. Proceedings of the National Academy of Sciences of the United States of America, 2012, 109, 17354-17359.	7.1	182
104	Size distributions and temporal variations of biological aerosol particles in the Amazon rainforest characterized by microscopy and real-time UV-APS fluorescence techniques during AMAZE-08. Atmospheric Chemistry and Physics, 2012, 12, 11997-12019.	4.9	187
105	Particle mass yield from <i>î²</i> -caryophyllene ozonolysis. Atmospheric Chemistry and Physics, 2012, 12, 3165-3179.	4.9	44
106	Using Elemental Ratios to Predict the Density of Organic Material Composed of Carbon, Hydrogen, and Oxygen. Environmental Science & Technology, 2012, 46, 787-794.	10.0	209
107	Organic Constituents on the Surfaces of Aerosol Particles from Southern Finland, Amazonia, and California Studied by Vibrational Sum Frequency Generation. Journal of Physical Chemistry A, 2012, 116, 8271-8290.	2.5	41
108	Biogenic Potassium Salt Particles as Seeds for Secondary Organic Aerosol in the Amazon. Science, 2012, 337, 1075-1078.	12.6	188

#	Article	IF	CITATIONS
109	Particle-Phase Chemistry of Secondary Organic Material: Modeled Compared to Measured O:C and H:C Elemental Ratios Provide Constraints. Environmental Science & Technology, 2011, 45, 4763-4770.	10.0	167
110	Stereochemical transfer to atmospheric aerosol particles accompanying the oxidation of biogenic volatile organic compounds. Geophysical Research Letters, 2011, 38, n/a-n/a.	4.0	18
111	Contrasting organic aerosol particles from boreal and tropical forests during HUMPPA-COPEC-2010 and AMAZE-08 using coherent vibrational spectroscopy. Atmospheric Chemistry and Physics, 2011, 11, 10317-10329.	4.9	30
112	Predicting the relative humidities of liquid-liquid phase separation, efflorescence, and deliquescence of mixed particles of ammonium sulfate, organic material, and water using the organic-to-sulfate mass ratio of the particle and the oxygen-to-carbon elemental ratio of the organic component. Atmospheric Chemistry and Physics, 2011, 11, 10995-11006.	4.9	297
113	Secondary Organic Material Produced by the Dark Ozonolysis of $\hat{I}\pm$ -Pinene Minimally Affects the Deliquescence and Efflorescence of Ammonium Sulfate. Aerosol Science and Technology, 2011, 45, 244-261.	3.1	69
114	Corrigendum to "An overview of the Amazonian Aerosol Characterization Experiment 2008 (AMAZE-08)" published in Atmos. Chem. Phys., 10, 11415–11438, 2010. Atmospheric Chemistry and Physics, 2010, 10, 11565-11565.	4.9	4
115	An overview of the Amazonian Aerosol Characterization Experiment 2008 (AMAZE-08). Atmospheric Chemistry and Physics, 2010, 10, 11415-11438.	4.9	170
116	A simplified description of the evolution of organic aerosol composition in the atmosphere. Geophysical Research Letters, 2010, 37, .	4.0	412
117	Rainforest Aerosols as Biogenic Nuclei of Clouds and Precipitation in the Amazon. Science, 2010, 329, 1513-1516.	12.6	541
118	Sources and properties of Amazonian aerosol particles. Reviews of Geophysics, 2010, 48, .	23.0	283
119	The Dynamic Shape Factor of Sodium Chloride Nanoparticles as Regulated by Drying Rate. Aerosol Science and Technology, 2010, 44, 939-953.	3.1	56
120	The 1-by-3 Tandem Differential Mobility Analyzer for Measurement of the Irreversibility of the Hygroscopic Growth Factor. Aerosol Science and Technology, 2009, 43, 641-652.	3.1	9
121	Mass spectral characterization of submicron biogenic organic particles in the Amazon Basin. Geophysical Research Letters, 2009, 36, .	4.0	171
122	Increased cloud activation potential of secondary organic aerosol for atmospheric mass loadings. Atmospheric Chemistry and Physics, 2009, 9, 2959-2971.	4.9	100
123	Cloud condensation nuclei in pristine tropical rainforest air of Amazonia: size-resolved measurements and modeling of atmospheric aerosol composition and CCN activity. Atmospheric Chemistry and Physics, 2009, 9, 7551-7575.	4.9	347
124	Loading-dependent elemental composition of $\hat{I}\pm$ -pinene SOA particles. Atmospheric Chemistry and Physics, 2009, 9, 771-782.	4.9	272
125	Global distribution of solid and aqueous sulfate aerosols: Effect of the hysteresis of particle phase transitions. Journal of Geophysical Research, 2008, 113, .	3.3	84
126	Particle mass yield in secondary organic aerosol formed by the dark ozonolysis of α-pinene. Atmospheric Chemistry and Physics, 2008, 8, 2073-2088.	4.9	175

#	Article	IF	CITATIONS
127	Nanosize effect on the hygroscopic growth factor of aerosol particles. Geophysical Research Letters, 2006, 33, .	4.0	100
128	Prompt deliquescence and efflorescence of aerosol nanoparticles. Atmospheric Chemistry and Physics, 2006, 6, 4633-4642.	4.9	158
129	Hydrothermal Synthesis of Pure α-Phase Manganese(II) Sulfide without the Use of Organic Reagents. Chemistry of Materials, 2006, 18, 1726-1736.	6.7	33
130	Nanosize Effect on the Deliquescence and the Efflorescence of Sodium Chloride Particles. Aerosol Science and Technology, 2006, 40, 97-106.	3.1	142
131	Apparent freezing temperatures modeled for several experimental apparatus. Journal of Geophysical Research, 2001, 106, 20379-20394.	3.3	13
132	Phase Transitions of Aqueous Atmospheric Particles. Chemical Reviews, 2000, 100, 3403-3454.	47.7	661